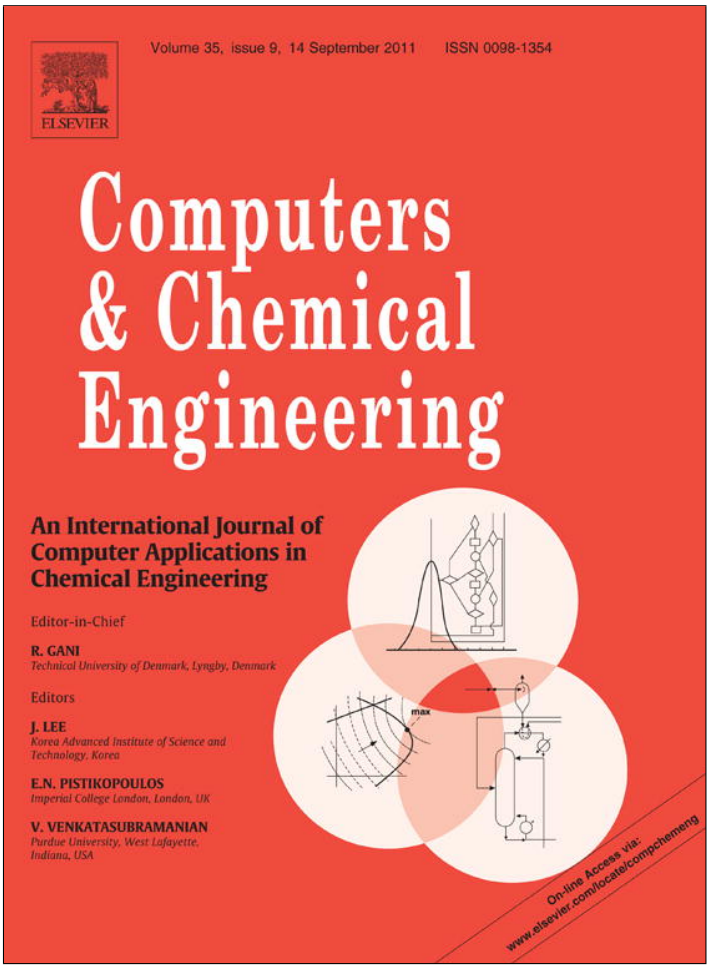

Computers and Chemical Engineering 35 (2011) 1863–1875

Contents lists available at ScienceDirect

Computers and Chemical Engineering

journal homepage: www.elsevier.com/locate/compchemeng

# Rigorous-simulation pinch-technology refined approach for process synthesis of the water–gas shift reaction system in an IGCC process with carbon capture

Juan M. Salazar[a], Urmila M. Diwekar[a,*], Stephen E. Zitney[b]

[a] Vishwamitra Research Institute, Center for Uncertain Systems Tools for Optimization and Management, Clarendon Hills, IL 60514, USA
[b] Collaboratory for Process & Dynamic Systems Research, National Energy Technology Laboratory, Morgantown, WV 26507, USA

ARTICLE INFO

*Article history:*
Received 28 October 2010
Received in revised form 22 April 2011
Accepted 1 May 2011
Available online 11 May 2011

*Keywords:*
IGCC system
Carbon capture
Chemical looping
MINLP process synthesis

ABSTRACT

Integrated gasification combined cycle (IGCC) technology is becoming increasingly more competitive among advanced power generation systems suitable for carbon capture. As an emerging technology, many different IGCC process configurations have been heuristically proposed to meet even more aggressive economic and environmental goals. One attractive design combines gasification with a water–gas shift (WGS) reaction system, pressure swing adsorption, and chemical-looping combustion (CLC) for $CO_2$ removal prior to feeding the fuel gas to the combined cycle for power production. The WGS reaction step is required to convert CO to $CO_2$ and the extent of conversion is determined by the degree of carbon capture required in the CLC step. As a first towards optimizing the overall energy efficiency of this IGCC process, we apply heat exchanger network synthesis (HENS) to the WGS reaction system. This particular part of the process was chosen because of its evident integration potential (steam required for the WGS reactions can be generated by recovering energy released by the same reactions) and the influence of some of the gasifier parameters (temperature and pressure) on its performance and on all the subsequent parts of the process. After generating alternative designs using Aspen Energy Analyzer (AEA), the HENS problem was formulated in the sequential-modular Aspen Plus simulator using a process superstructure approach and solved by mixed integer nonlinear programming (MINLP) algorithms. The HENS capability is implemented as CAPE-OPEN (CO) compliant unit operation and makes use of MINLP algorithms, namely Generalized Bender's Decomposition (GBD), Outer Approximation (OA), Equality Relaxation (ER), Augmented Penalty (AP), and Simulated Annealing (SA). This MINLP-based HENS was used in the CO-compliant Aspen Plus simulator to obtain a design for the WGS reaction system that provided a cost of energy for the IGCC system with $CO_2$ capture that was 28% lower than the base case.



## 1. Introduction

In the past years, large efforts have been invested in the development of advanced power generation systems that meet today's energy needs while achieving a sustainable equilibrium between economic, environmental and social performance (El-Sayed, 1999). The level of $CO_2$ emissions is one of the performance parameters for fossil-fueled power systems where such equilibrium needs to be reached. Integrated gasification combined cycle (IGCC) systems with efficient post-gasification technologies offer a potential opportunity for providing low $CO_2$ emission levels at economically feasible conditions (Doctor, Molburg, & Thimmapuram, 1996).

In this paper, we consider an IGCC configuration that combines several post-gasification technologies, including a water–gas shift (WGS) reaction system, pressure swing adsorption (PSA), and chemical-looping combustion (CLC). Using steam, the WGS reactors convert large amounts of CO produced at the gasification step into a $CO_2$ and $H_2$ mixture. The PSA system produces a hydrogen-rich fuel which is sent to the combined cycle to generate power. The CLC system oxidizes the remaining CO and methane in the flue gas stream to generate sequestration-ready $CO_2$ stream and a gas stream which is sent to the combined cycle to produce electricity (Hoffman, 2005). These post-gasification technologies require an important effort to integrate them into the IGCC flowsheet in an optimal way. This problem is addressed in the present work.

While pinch analysis is a widely recognized tool for the design of heat exchanger networks in chemical processes, it has not been applied routinely to conventional pulverized coal power cycles, which involve a considerable number of operations for heat exchange. Early contribution in this area is the work by Linhoff and Alanis (1989). More recent works by Harkin, Hoadley, and Hooper (2009) applied pinch techniques to evaluate the possibilities of heat recovery from energy systems with carbon capture technologies. Farhad, Saffar-Avval, and Younessi-Sinaki (2008) combine

* Corresponding author. Tel.: +1 630886 3047.
*E-mail address:* urmila@vri-custom.org (U.M. Diwekar).

0098-1354/$ – see front matter © 2011 Elsevier Ltd. All rights reserved.
doi:10.1016/j.compchemeng.2011.05.001

**Nomenclature**

| | |
|---|---|
| $\Delta$ | difference in costs of initial and perturbed solution |
| $A$ | coefficient from CE cost estimation |
| $B/B$ | matrix with coefficients of binary variables in inequality constraints/coefficient from CE cost estimation |
| $C/C$ | maximum number of $T$ values with the same cost/coefficient from CE cost estimation |
| CE | chemical engineering coefficient for cost estimation |
| $C_j$ | cost of unit $j$ |
| $f(x)$ | non-linear component of the objective function for the MINLP problem |
| $F_{14}$ | mass flow (lb/h) at splitter 14 |
| $g(x)$ | non-linear component of inequality constraints |
| $h(x)$ | non-linear equality constraints (corresponding to mass and energy balances) |
| $K$ | maximum total number of perturbations (moves) in SA algorithm per value of $T$ |
| $O_i$ | artificial decision variables to extract information on the constraints for the master problem in MINLP |
| $P$ | coefficient from CE cost estimation |
| $S$ | initial solution for the decision variables in SA algorithm |
| $S'$ | solution for the decision variables in SA algorithm after perturbation of $S$ |
| $T$ | parameter for acceptance probability in SA algorithm (temperature) |
| $T_{freeze}$ | final value of parameter $T$ |
| $T_{ini}$ | starting parameter |
| $U$ | large number |
| $x$ | vector of continuous decision variables |
| $X_i$ | dummy decision variables corresponding to each $O_i$ |
| $y$ | vector of binary decision variables |
| $Z$ | objective function of the MINLP problem |

pinch technology and exergy analysis for the design of feed water heaters taking into account other energy consumers such as pumps and compressors. On the IGCC processes Diwekar, Grossmann, and Rubin (1992) studied the gas cleaning alternatives of an IGCC process by formulating a mixed integer non-linear programming (MINLP) problem and employing a process model in Aspen Plus. In the same year (1992) Vlaswinkel (Vlaswinkel, 1992) studied a combination of exergy analysis and pinch technology for the optimization of an IGCC spreadsheet-based model. A more recent study have addressed heat and mass process integration in IGCC systems (Wang, Qiu, Wu, & Li, 2010) but avoiding the employment of pinch technology for the heat integration part. Gadalla et al. (Emun, Gadalla, Majozi, & Boer, 2010; Gadalla, Emun, Majozi, & Jiménez, 2009) used an Aspen Plus model of an IGCC process to optimize the process through sensitivity analysis and suggested some potential opportunities for heat integration. Madzivhandila, Majozi, and Zhelev, 2009 proposed an integrated flowsheet that employs all the syngas streams to generate steam for the plant substituting the boiler and the typical HRSG section, the flowsheet is proposed based on a pinch technology software named Super Target version 6.0. A very recent contribution is a complete study of the integration and cost evaluation of an IGCC process fed with refinery heavy residues is presented by Domenichini, Gallio, and Lazzaretto (2010); the process comprises post gasification technologies as WGS and PSA and proposes a single flowsheet based on pinch technology integrating the steam generation with cooling operations in WGS section and waste treatment sections.

From the above-mentioned contributions one can infer that pinch technology is an appropriate tool for the process integration of new IGCC technologies. One or several heat exchange networks can be formulated by existing software packages or simply by combining the pinch technology guidelines with heuristics. Aspen Energy Analyzer (AEA) is a computer program that provides a tool for heat exchanger network synthesis; this tool generates several alternative designs through an algorithmic approach based on the pinch technology guidelines. However, AEA uses models which are linear in nature and when the resulting configurations are simulated with the Aspen Plus their performance is considerably different to the supposedly optimal originally predicted by AEA. This calls for a coupled approach where AEA analysis is used to generate various flowsheet configurations and then Mixed Integer Nonlinear Programming (MINLP) process synthesis approach is used for more detailed analysis to obtain optimal flowsheet configuration and design.

This paper makes use of AEA for the generation of alternative designs based on pinch technology. The MINLP problem is then solved based on the rigorous Aspen Plus model of an IGCC process with WGS reaction and chemical looping as post-gasification technologies.

## 2. Process description and background

For this work the entire process has been modeled in Aspen Plus according to the work by Hoffman (2005), the reader is encouraged to refer to Hoffman work for details and assumptions related to this model. The integrated gasification combined cycle (IGCC) process is typically comprised of two main parts: the gasifier island and the power island. The gasifier carries out the reaction of coal with oxygen and water to produce mostly syngas (CO and $H_2$); however, other reactions such as partial oxidation of coal, water–gas shift reaction and, synthesis reactions and reactions involving the interaction of water and coal may take place. Other coal components as nitrogen and sulfur also react producing ammonia and $H_2S$. For the coal gasification one reactor decomposes the stream of coal into its elemental constituents (C, $H_2$, $N_2$, $O_2$, S, $H_2O$ and ash as a yield reactor) and a second reactor generates the fuel composed of $CH_4$, $H_2$, CO, $NH_4$, $H_2S$ and $CO_2$ (in addition to unreacted $N_2$, $O_2$, $H_2$ and $H_2O$) by minimizing the total Gibbs free energy of the system (Gibbs reactor). In addition to the assumed products of the reactions, the operating conditions of the gasification system are also specified as 1200 °C and 450 psia (31 bar). The flowsheet diagram of the gasification process is shown in Fig. 1.

Sulfur and ammonia removal are also part of the gasifier island. In the gas cleaning step, $H_2S$ is removed by an absorption unit using methanol or glycol. The removal of ammonia is carried out with a reactive absorption process on sulfuric acid; both separations are modeled in Aspen Plus as one single unit or simple component separator.

The power island is comprised of the gas turbine that generates electricity from the outlet stream of combustion system and a typical high pressure (HP), intermediate pressure (IP) and low pressure (LP) steam turbine that uses steam from the heat recovery steam generator (HRSG).

Inclusion of post-gasification processes to facilitate the $CO_2$ capture and subsequent sequestration has been proposed by Hoffman (2005). The process is comprised of four main areas: coal gasification, water gas shift reaction, sorbent energy transfer system (SETS), and power generation. The general representation of the process is shown in Fig. 2. The gasification and power generation systems have been previously described; therefore, the subsequent parts of this section include the main features of the two post-gasification

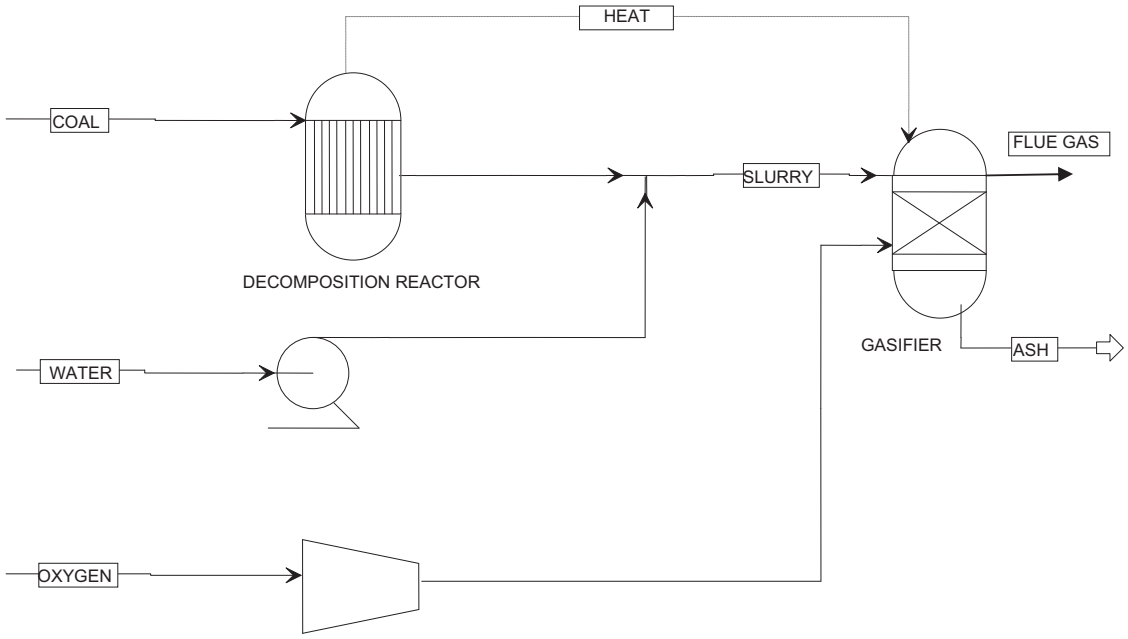


**Fig. 1.** Aspen plus representation of gasification process.

technologies namely the water–gas shift reaction and the chemical looping (SETS) systems.

## 3. Water–gas shift reaction system

The products of the coal gasifier are fed to the water–gas shift (WGS) reactor section for oxidation of the CO with the simultaneous production of hydrogen. The main reaction is presented in Eq. (1).

$$H_2O + CO \leftrightarrow CO_2 + H_2 \quad (1)$$

The process is simulated with two adiabatic Gibbs reactors in series where all the components of the synthesis gas were considered as products except $CH_4$ which was considered as an inert. Steam is mixed with the synthesis gas prior to entering the first reactor. Intermediate heat exchangers are used to cool down the reactor products and generate steam. The flowsheet diagram of this part of the process is presented in Fig. 3. This section of the process is finished with a pressure swing adsorption (PSA) unit to purify the hydrogen that is fed to the gas turbine; the unit is modeled as a simple component separator.

### 3.1. Sorbent energy transfer system (SETS) based on chemical looping combustion (CLC)

To complete the combustion of the CO remaining from the WGS reaction train, the $CH_4$ from the gasification (which passed inert through the WGS) and the hydrogen that was not separated by the PSA, a sorbent energy transfer system (SETS) was proposed (Hoffman, 2005). SETS was previously formulated for a natural gas combined cycle (NGCC) (Yu, Corripio, Harrison, & Copeland, 2003) as an efficient way to generate sequestration-ready $CO_2$ and it is expected to be a suitable option for the outlet gases of an IGCC-WGS system.

SETS employs the basic principle of chemical looping combustion (CLC) where a reduction reactor is fed with the fuel (CO, $CH_4$ and $H_2$) and a sorbent (metal oxide). The metal in the sorbent is

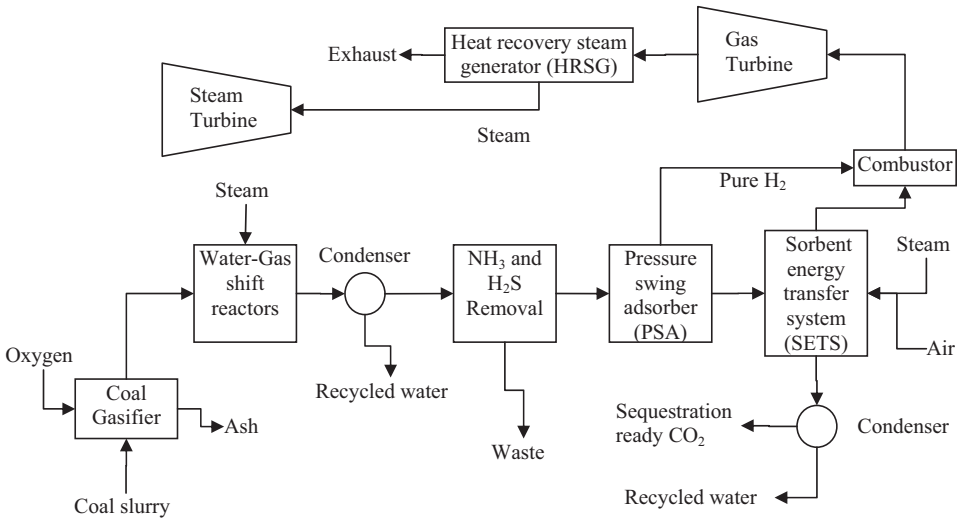


**Fig. 2.** General diagram of gasification process adapted from Hoffman (2005).

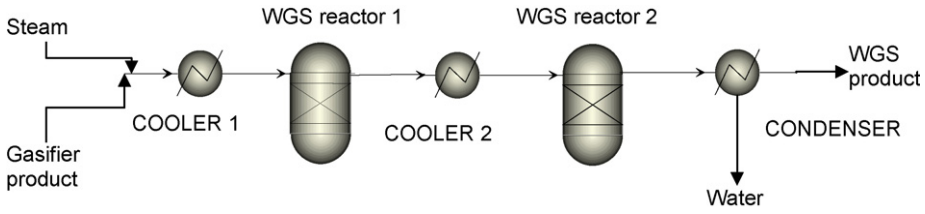


**Fig. 3.** Water gas shift reactor section without heat exchange integration.

reduced to a lower valence or to its metallic form by the oxidation of the fuel to $CO_2$ and water. Then, the reduced sorbent is fed to an oxidation vessel along with air to recover its original form (an oxide). In this way, the process avoids the direct contact of the fuel with air and the dilution of $CO_2$ with air $N_2$ and excess $O_2$. The process flowsheet is shown in Fig. 4.

Due to lack of experimental data, the main assumption in the simulation of this part of the process is that reduction reactor, oxidation reactor, and combustion chamber behave as adiabatic Gibbs reactors with equilibrium reactions. The reader should notice that these assumptions can be modified to any other experimentally-validated approaches and the results of the simulations will vary; the experimental validation of these models is out of the scope of this work. Sorbent employed at this model is a mixture of 25% NiO in $Al_2O_3$. The gas product of the reduction vessel contains highly pure $CO_2$ that needs to be cooled down to condensate the water and to produce steam. This steam can bring the energy lost from the $CO_2$ and water coming out of the reduction reactor back into the system. It is considered that 1 mol of sorbent-oxidized $CH_4$ (at reduction vessel) can be returned as 3 mol of steam, 1 mol of $H_2$ and CO return as 1 mol of steam respectively. The outlet gas exiting the oxidation vessel along with the $H_2$ from the PSA are combusted and go through a gas turbine to generate energy. The gas subsequently goes through the heat recovery steam generation (HRSG) to generate more power.

### 3.2. Heat exchanger network synthesis

Although many parts of the new process described in the previous sections and presented in Fig. 2 display interesting opportunities for heat integration, this work is concentrated in the heat integration of the WGS reactor train since this part of the process is strongly influenced by operation conditions of the gasifier and strongly influences downstream processes; however, the methodology expressed in this paper can be applied to a global integration of the process.

A widely known and employed technique for the heat integration of new and existing processes is the pinch analysis (Linhoff et al., 1982). Pinch analysis is often employed, along with mathematical programming techniques, for reducing capital and operational costs by integrating hot and cold streams to minimize the use of external utilities or to minimize the number of units in a heat exchange network. Initially, the methodology calculates the energy targets which are the minimum requirements of utilities by a particular set of hot and cold streams. Another important piece of information that is defined with this initial step is the pinch point; it identifies hot and cold streams in the process that will need to exchange heat under a temperature difference equal to the minimum difference allowed to be able to accomplish a complete heat recovery.

These parameters are represented in the "composite curve", a plot of temperature versus enthalpy of linear representations (at constant heat capacity) for hot and cold streams. The targets and the pinch point provide the designer with the performance boundaries before the first design is formulated and offer important guidance to formulate designs that can be close to the ideal or boundary design. Aspen Energy Analyzer (AEA) yields the composite curve, the pinch diagram and a set of alternative designs based on data about the streams that need to be integrated. Although, AEA uses linear representation of problem, in reality, the problem is nonlinear and includes integer decisions indicating presence or absence of a unit converting the problem into a Mixed Integer Nonlinear Programming (MINLP) problem that is simplified into a Mixed Integer Linear Programming (MILP) problem by AEA. In this work, CAPE-OPEN compliant capabilities for MINLP process synthesis have been implemented to solve this problem.

### 3.3. CAPE-OPEN compliant MINLP process synthesis capabilities

Optimization approach to process synthesis involves defining a search space as a superstructure that combines candidate flowsheet structures (which may be based on preliminary or heuristic screening) and this superstructure can be modeled in a sequential

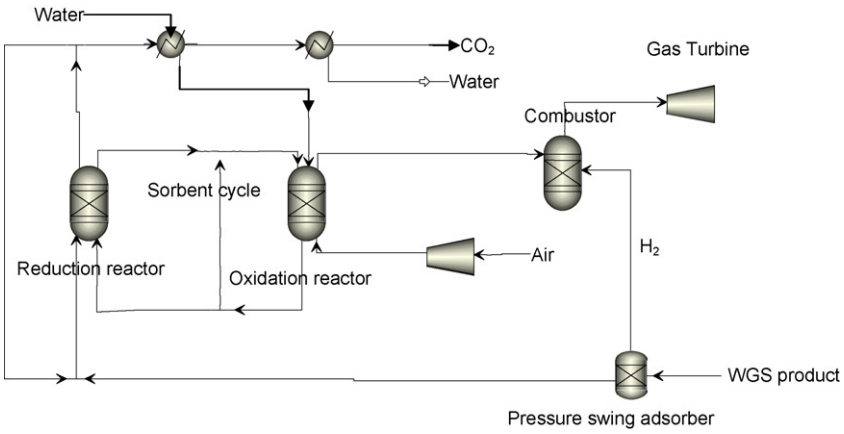


**Fig. 4.** Model of SETS and gas turbine.

modular simulator as Aspen Plus. The superstructure is the object of a Mixed Integer Non-linear Programming (MINLP) problem of the form given in Eq. (2) where the continuous variables $x$ represent flows, operating conditions, and design variables and the binary variables $y$ denote the potential existence of process units. This selection of units is defined by splitters in the superstructure model that direct the mass flow of the streams related to such units. In Eq. (2) $f$ represents annualized costs of the units based on size parameters and also the operating costs divided by the energy generated in kW; $h$ represent all the mass and energy balances calculated by the superstructure model; $g$ are nonlinear functions of capital costs for each unit; and $B$ is a matrix of large positive number and zeros that will guarantee that $g$ vanishes when the corresponding $y$ takes the value of 0, as well as all the feasibility constraints

$$\begin{aligned} &Z = f(x)(\text{annualized capital cost} + \text{operational cost})\ \text{s.t.}\\ &h(x) = 0(\text{mass and energy balances in the superstructure})\\ &By + g(x) \le 0(\text{when } y = 0 \quad \text{then } g(x) = 0) \quad y \in [0,1]; x \in R \end{aligned} \tag{2}$$

The problem formulated in Eq. (2) can be solved using mathematical programming methods commonly known as MINLP methods. The generalized MINLP methods for process synthesis are based on the so-called Generalized Bender's Decomposition (GBD) and Outer Approximation (OA) and their variants. GBD and OA methods are based on the information that can be obtained about the objective function and constraints as well as their derivatives, and they are gradient-based methods. Gradient-based methods present difficulties when solving non-convex problems which are very common in process synthesis applications. Alternative to gradient-based methods, combinatorial probabilistic methods can be employed to solve MINLP problems. These methods make their search for the optimal solution based on mimicking some natural process as metal annealing or genetic evolution (Diwekar, 2008).

#### 3.3.1. Algorithms

We use two algorithms in this paper to solve the MINLP problem, the GBD/OA/ER/AP algorithm and the Simulated Annealing (SA) algorithm. These algorithms are described briefly below.

### 3.4. GBD/OA/ER/AP

The GBD and OA algorithms for solving the above mentioned MINLP problems consist of solving a non-linear programming (NLP) sub-problem at each subsidiary or minor iteration (with binary or 0–1 variables fixed) and a Mixed Integer Linear Programming (MILP) master problem at each primary or major iteration. The role of the NLP sub-problem is to optimize the continuous variables and provide an upper bound to the optimal MINLP solution. On the other hand, the role of the MILP master problem is to predict a lower bound to the MINLP solution as well as new values of binary variables. The predicted lower bound increases as the cycle of major iterations proceeds, with the search terminated when the predicted lower bound coincides or exceeds the upper bound. The specific variant that is used in this work is called GBD/OA/Equality Relaxation (ER)/Augmented Penalty (AP) function algorithm (Diwekar, Frey, & Rubin, 1992; Diwekar, Grossmann, et al., 1992).

### 3.5. Simulated annealing

As noted previously, probabilistic methods are based on analogies with physical phenomena as metal annealing or genetic evolution. Algorithms based on annealing are called simulated annealing (SA) with this work primarily focused on one of its applications. In the annealing process, metals undergo slow cooling processes through sequence of temperature steps. Once the thermal equilibrium is reached at each step, atoms are self organized in lattices whose energy is minimal. Analogously, the optimization problem required to reach a configuration (set of discrete decisions) whose cost is minimal. Each configuration comprises both binary and integer variables: the former define the existence of operating units and the latter correspond to selected discrete values of the continuous variables. The SA algorithm starts with an initial configuration and calculates its corresponding cost. Subsequently, a move generator provides a random configuration; if the cost of the second configuration is lower than the initial one (downhill move), the move is accepted. Otherwise (uphill move) the configuration can be accepted with probability exp $(-(\text{cost2} - \text{cost1})/T)$, where $T$ is temperature. The reader should be aware that this temperature is a parameter that allows defining the probabilities in which the uphill moves are accepted; the acceptance probability decreases as the pseudo-temperature parameter does which is analogous to the annealing process. This procedure is repeated at each temperature level until equilibrium is reached (no significant changes in costs for a certain number of generated moves) and the general algorithm stops when a certain freezing temperature is reached (Diwekar, 2008).

### 3.6. Implementation in a sequential modular simulator

#### 3.6.1. GBD/OA/ER/AP

The GBD/OA/ER/AP algorithm requires the transfer of information about the constraints and objectives from the NLP problem to the master problem. The master problem is a linearized version of the NLP problem. When a sequential modular simulator is employed as the model (constraints), most of the variables are implicit within the black-box models making it impossible to transfer information about the variables to the master problem. This restriction was addressed by including new decision variables and constraints that involve some of the implicit variables (Diwekar, Frey, et al., 1992; Diwekar, Grossmann, et al., 1992). It is important that the master problem have enough information to obtain good solutions. In process synthesis problems the information of units to which flow is zero cannot be obtained. To circumvent this problem a decomposition strategy involving various NLP subproblems is employed (Diwekar, Frey, et al., 1992; Diwekar, Grossmann, et al., 1992). Therefore, along with implicit variables and constraints, it is important to identify initial flowsheet and subproblems to ensure all units are covered. In general the optimization of the superstructure involves the following steps:

1. Identifying implicit variables of the flowsheet.
2. Identifying the continuous decision variables, their initial values and their bounds.
3. Identifying initial flowsheet and subproblems so that information about all units is available to the master problem.
4. Identifying constraints (including implicit constraints).
5. Identifying the relationship between binary variables and continuous variables to be supplied to the MILP master problem.
6. Provide analytical derivative information for implicit variable based derivatives as suggested by Diwekar and Rubin (1993).

The MINLP process synthesis is implemented as a CAPE-OPEN compliant capability in Aspen Plus. This capability allows for specifying the superstructure, initial flowsheet, and subproblems. Iterative calculations between the master problem and subproblems are carried out automatically using a batch file. The MINLP capability generates calculator blocks for ASPEN which are used to communicate between the MINLP algorithm and the flowsheet. For details of this capability, please refer to (Diwekar, 2010a).

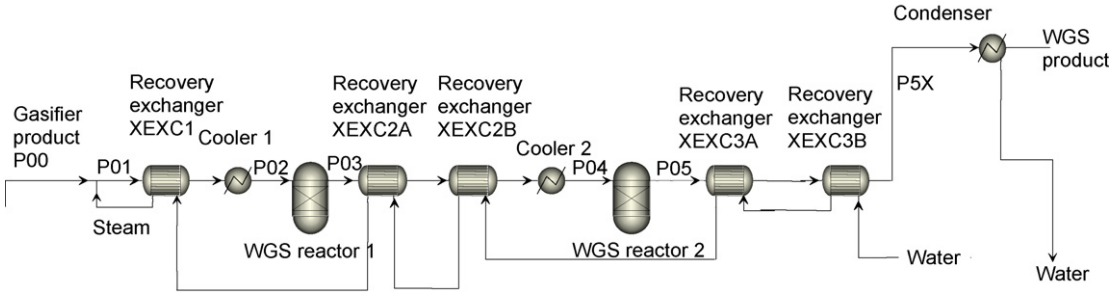


**Fig. 5.** Original heat integration (base case).

### 3.7. Simulated annealing

Simulated annealing (SA) has not been explicitly designed to handle continuous variables; however, in contrast to the GBD/OA/ER/AP algorithm, it can handle both binary and integer variables. Hence, binary variables are assigned to the discrete variables of the MINLP problem and integer variables are assigned to a discrete version of the continuous variable's range. To guarantee that this discrete set covers homogeneously the continuum without scaling up the number of nodes with number of variables, an efficient sampling technique is employed namely Hammersly Sequence Sampling (HSS) (Kalagnanam & Diwekar, 1997). The move generator routine is employed to perturb the decision variables (in both binary and integer variables) with the characteristic of a Markov chain, i.e. each move in the decision variables domain depends only on their present values. The steps of the SA algorithm are described (Diwekar, 2008):

1. Obtain an initial configuration $S$ (solution flowsheet).
2. Select an initial temperature $T_{ini}$ and a freezing temperature $T_{freeze}$.
3. Perform the following loop while $T > T_{freeze}$.
   a. Perform the following loop $K$ times ($K$ is the maximum number of moves per each temperature level)
      i. Generate a move $S'$ by perturbing $S$.
      ii. $\Delta = \text{Cost}(S') - \text{Cost}(S)$.
      iii. Accept the move ($S = S'$) if $\Delta < 0$ or $n \leq \exp(-\Delta/T)$. where $n$ is a random number.
      iv. Determine the number of times that the moves have been accepted and rejected.
      v. Determine if $K$ has been reached.
   b. No significant change in last $C$ temperature levels, go to step 4.
   c. Decrease $T$.
4. Solution reached.

The SA is also implemented in Aspen Plus as a CAPE OPEN compliant capability (Diwekar, 2010b).

## 4. Results and discussion

### 4.1. Aspen Energy Analyzer and superstructure

Within the IGCC with chemical looping combustion process, the heat exchange network of the WGS reactor section was identified as a synthesis problem whose solution can be achieved with the combination of the AEA tools and two MINLP synthesizers in Aspen Plus simulator. The original work that studied this process (Hoffman, 2005) identified three variables that are influential in the process economics: the gasifier temperature and pressure and the steam to CO ratio that is fed to the WGS reactors. These conditions affect the performance of the WGS and are restricted by the conditions of the SETS (chemical looping system), for this reason, the heat integration of the WGS reactor system is considered an important part of the synthesis. The original model suggests an integrated heat exchange network as shown in Fig. 5. The cold water is initially heated with two units (XEXC3A and B) with the gas stream coming out of the WGS reactor 2 (WGS2). This water is then evaporated in another set of heat exchangers (XEXC2A and B) with the heat from the WGS reactor 1 outlet, the steam is overheated by XEXC1 with the gasifier product. Additionally, two coolers are required to completely remove the heat from the WGS reactor product stream. The main purpose of the heat exchanger network synthesis problem is to evaluate whether this is an optimal configuration. Aspen Energy Analyzer (AEA) provides useful tools for the evaluation and formulation of heat exchanger network synthesis.

To formulate a heat exchanger network synthesis problem, AEA extracts the streams that potentially can be used for the heat integration from the original non-integrated simulation. As shown in Fig. 5, the extraction of the data requires some modifications such as the inclusion of isothermal mixers to guarantee the consideration of the heat exchange that occurs when mixing stream "STEAM" with "P00" and the removal of the water condenser (COND1) as a potential integration alternative. The flowsheet where AEA extracted the stream data from is shown in Fig. 6.

The streams available for heat release are identified as P01 to P02, P03 to P05 and P05 to P5X, the set of streams recognized as the set of hot streams. The set of cold streams comprises the stream of water at ambient temperature to water at saturation temperature, the saturated liquid to saturated steam and the saturated steam to overheated steam. The characteristics of the hot streams were extracted from the simulation directly to the Aspen Energy Analyzer. On the other hand, only the final characteristics of the overheated steam stream were extracted directly from the simulation. The characteristics of the intermediate liquid and vapor streams were manually entered to the AEA. For this purpose, the temperature at which the steam evaporation occurs is assumed to be 236 °C the temperature at which the WGS reactants must enter the reactors. Therefore, the evaporation stream was assumed to undergo a small temperature change (236.3–236.5 °C) and a large enthalpy change. Table 1 shows the assigned names and temperatures for the hot and cold streams. As previously noted, Table 1 and Fig. 5 illustrate that the mixer located immediately upstream the first reactor is a non isothermal mixer; this condition makes it suitable to be part of the heat integration problem. To include it as part of this problem, two more streams are added, one as P00 (stream coming out of the gasifier) to stream 2 at 633.5 °C to make the mixer an isothermal mixer and a second stream that corrects the mixing enthalpy change to obtain the original temperature of stream P01 (initially calculated by the non isothermal mixer and also equal to 633.5 °C) as shown in Fig. 6.

Therefore, information contained in Table 1 can be represented as an integration scenario within the AEA environment whose composite curve is shown in Fig. 7.

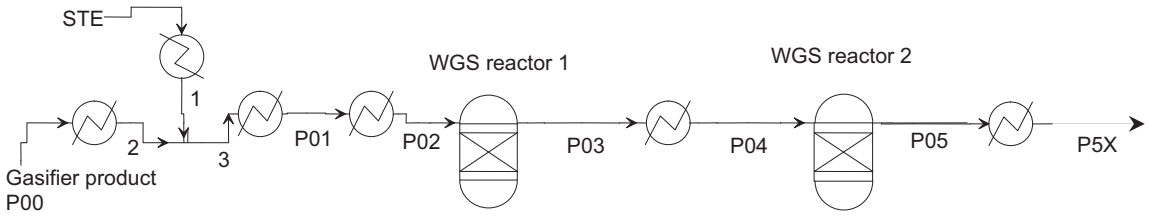


**Fig. 6.** Flowsheet for the extraction of stream information.

**Table 1**
Stream definition for the heat exchanger network synthesis problem.

| Stream | Heat capacity flowrate (kJ/°C h) | Initial temperature (°C) | Final temperature (°C) |
|---|---|---|---|
| P01 to P02 | $7.284 \times 10^5$ | 633.5 | 236.3 |
| P03 to P04 | $7.429 \times 10^5$ | 426.6 | 236.3 |
| P05 to P5X | $2.188 \times 10^6$ | 252.8 | 176.7 |
| R1 to R1D (liquid water) | $1.014 \times 10^6$ | 35 | 236.3 |
| R1D to STE (vaporization) | $1.238 \times 10^9$ | 236.3 | 236.6 |
| STE to 1 (overheating) | $4.465 \times 10^5$ | 236.6 | 633.5 |
| P00 to 2 | $3.157 \times 10^5$ | 1200 | 633.5 |
| 3 to P01 | $7.544 \times 10^5$ | 631.5 | 633.5 |

The targets for this set of streams are zero for the heating requirements and $1.83 \times 10^7$ kJ/h of cooling requirements. Fig. 7 shows the offset between the hot and the cold lines at low values of enthalpy. These results suggest that an ideal design will be able to generate all the steam required for the WGS reactors but not all of the heat released by the reactions can be rejected in that way.

The base case shown in Fig. 5 was included in this analysis and is represented in Fig. 8 where a small amount of heat is required to be added to one of the mixer streams to compensate the numerical differences in the data extraction process. To understand this representation the hot streams are shown as left-to-right arrows and the cold streams as right-to-left. The cold lines in the upper part of the figure are cold utilities and can be linked to hot streams with a line that represents the heat exchange between hot streams and the cooling utilities, similarly the bottom hot lines are hot utilities that are connecting cold streams and the heating utility. The remaining linking lines represent heat exchangers involving hot and cold streams, i.e. the integrated heat exchangers.

For the solution of the heat integration problem, the AEA uses this information along with heat transfer coefficients and economics to generate a set of designs for which the costs are minimal.

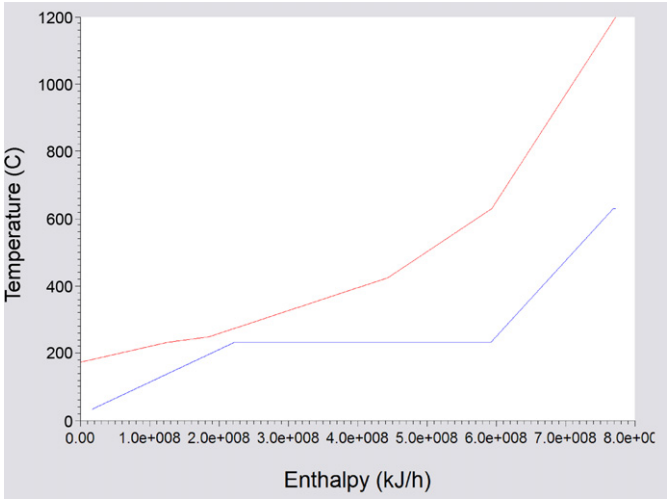


**Fig. 7.** Composite curve for the data extracted by AEA (temperature scale from 0 to1200 °C).

AEA employs a linear programming algorithm to provide these designs based on linear models for the energy balance of the heat exchangers. One of these alternative designs (Design 1) is shown in Fig. 9. However, it has been found that linear approximation of the energy balances may be inaccurate and therefore the proposed designs are not necessarily optimal. Table 2 shows the cooling and heating requirements reported by the AEA and it can be seen that they are considerably different to those reported by Aspen Plus simulations of such designs. Therefore, these designs were used simply as alternatives combined in a superstructure that was analyzed and optimized with the GBD/OA/ER/AP and SA algorithms previously described and implemented as CAPE-OPEN capabilities.

The superstructure was created through a set of splitters and mixers which connect the three alternative designs formulated by AEA. It should be remembered that these three alternatives when combined in a superstructure can generate a large number of alternatives for process synthesis. With the employment of appropriate thermodynamic and transport properties the Aspen Plus simulation of the superstructure provides realistic results of the mass and energy balances for the designs and other resulting potential combinations (many units are common to all or two of the designs and therefore the superstructure may contain several other combinations that may provide improved performance parameters) avoiding the simplifications of the AEA optimization. Fig. 10 displays a small part of the superstructure that comprises units from the three potential designs. Splitter 1 (SPL1) directs stream R1 towards R-1-1 or R1-4-7, the former belongs to designs 1 and 3 and the latter to Design 2; when directed towards R1-4-7 the water flow proceeds towards units R1-4-8 and R1-4-9 which all belong to Design 2. On the other hand, splitter 2 (SPL2) directs the stream towards R1-4-1 or R1-4-4 that belong to Design 1 and Design 3 respectively, the flow of Design 1 goes through R1-4-2 and R1-4-3 towards a mixer where it comes across with the streams that

**Table 2**
Comparison of AEA and Aspen Plus simulations.

| Design | Aspen EA | | Aspen Plus simulation | |
|---|---|---|---|---|
| | Heating 10E6 kJ/h | Cooling 10E6 kJ/h | Heating 10E6 kJ/h | Cooling 10E6 kJ/h |
| 1 | 10.3 | 39.1 | 12.5 | 42.4 |
| 2 | 10.3 | 30.1 | 8.7 | 47.4 |
| 3 | 10.3 | 37.3 | 14.9 | 34.0 |

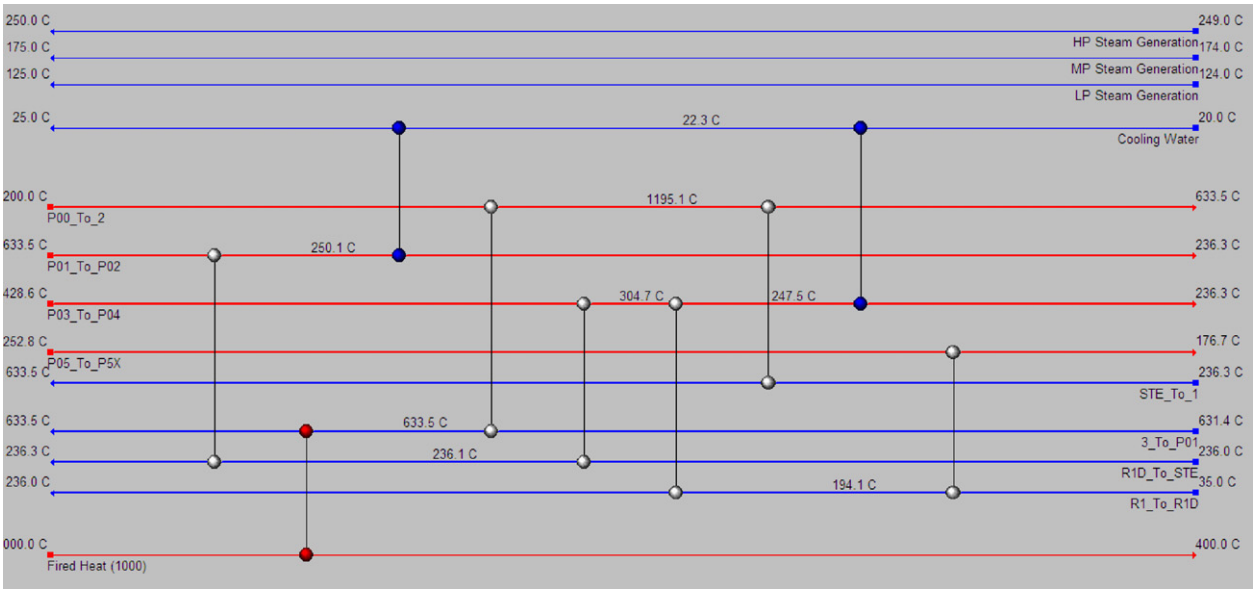


**Fig. 8.** Simplified representation of base case design from AEA.

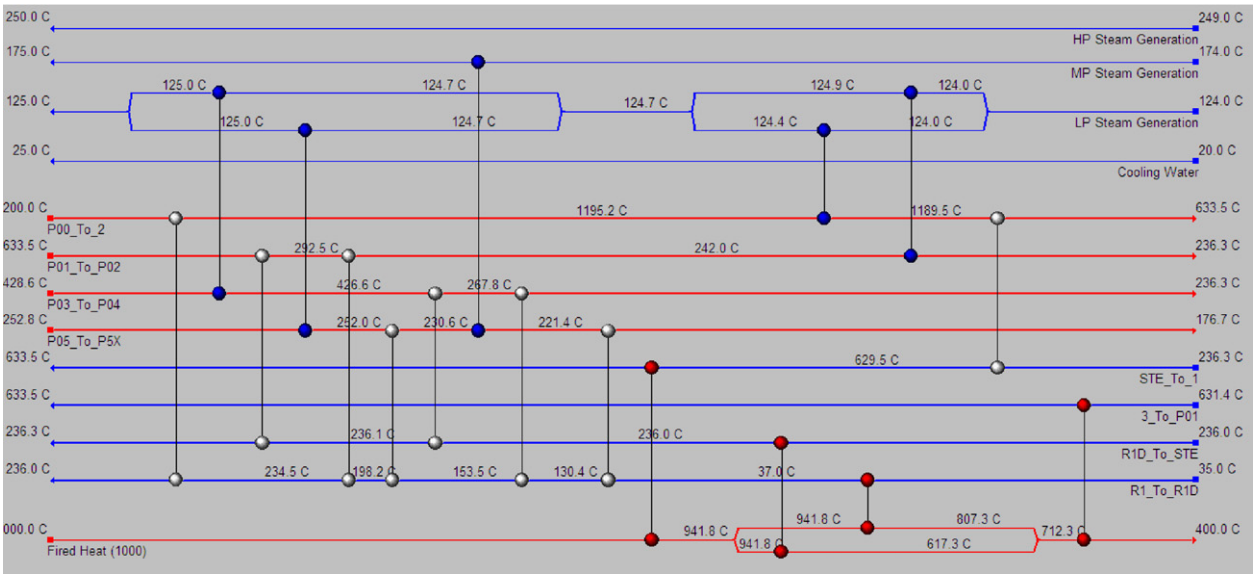


**Fig. 9.** Simplified representation of the alternative design suggested by AEA.

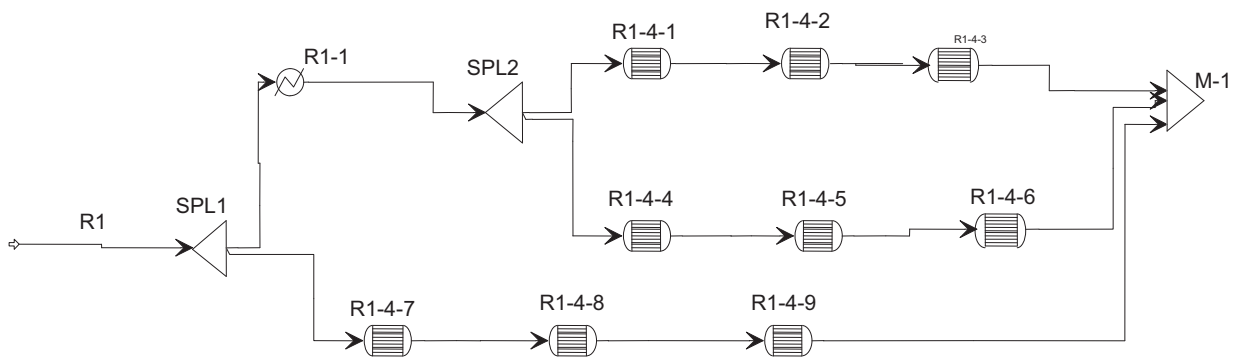


**Fig. 10.** Splitter-mixer arrangement to build a superstructure.

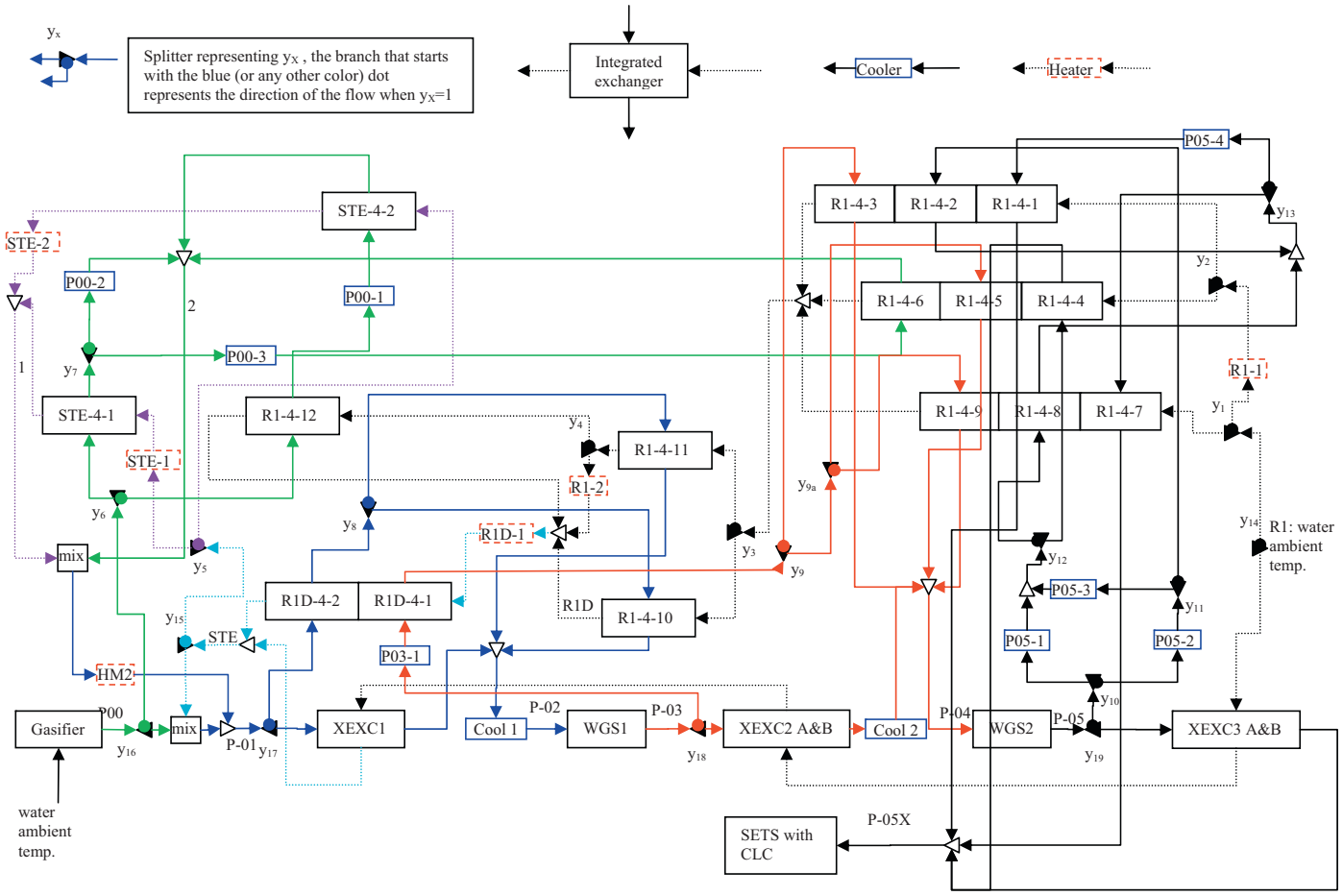


**Fig. 11.** Superstructure of the WGS heat integration for an IGCC system with chemical looping.

are part of Design 2 (from units R1-4-5 and R1-4-6) and Design 3. Splitters 1 and 2 should choose only one of the streams to evaluate only one design at a time, therefore only one of the inlet streams of mixer (M-1) should have a nonzero flow rate.

To select a particular configuration, an appropriate value (1 or 0) should be given to the mass flow fraction specification of each of the 20 splitters comprising the complete superstructure. The master problem in the GBD/OA/ER/AP algorithm and the random move generator in the SA algorithm provide these mass flow fractions in order to run the simulation of any possible configuration. Each splitter has one binary variable $y$ associated to it; for instance, the specification of $y_1 = 1, y_2 = 1, y_3 = 1, y_4 = 1, y_5 = 1, y_6 = 1, y_7 = 1, y_8 = 1, y_9 = 1, y_{9a} = 0, y_{10} = 1, y_{11} = 1, y_{12} = 0, y_{13} = 1, y_{14} = 1, y_{15} = 1, y_{16} = 1, y_{17} = 1, y_{18} = 1$ and $y_{19} = 1$ will evaluate Design 1 since each splitter will assign mass flow fraction equal to 1 for the streams that connect the units comprising only Design 1. The base case represented in Fig. 5 was also included in the superstructure which can be obtained when $y_{14} = y_{15} = y_{16} = y_{17} = y_{18} = y_{19} = 0$. It should be noted that the base case was not in the best designs resulted from AEA analysis. Fig. 11 shows a simplified scheme of the complete superstructure, with all the splitters and mixers included; however, some operating units are summarized as the post combustion units.

As stated previously, each splitter is controlled by one binary variable and the flow is directed depending on the value this variable takes. The process starts with the gasifier, whose outlet stream is P00. This stream is mixed with STE and the combination is cooled down to P-02 which enters the first water–gas shift reactor or WGS1. Outlet from this unit is P-03, which is cooled down to stream P-04, to be fed to the second WGS reactor named WGS2. Finally stream P-05 is again cooled down to become P-05X which is fed to the post combustion SETS with chemical looping combustion. The gasifier outlet undergoes cooling with the generation of the steam that starts with stream R1 and finishes with streams STE or 1. Water flow is represented by dotted lines and gas flow with solid lines. As cold streams are connected in series (they all are part of same stream that generates steam for WGS reaction), the direction of its flow is used as a guide to formulate the logical binary constraints. The aim is to guarantee that there is flow through all the streams heating a particular flow path chosen by splitters on the cold stream. Initially as splitters 1 and 2 are placed in cascade they may generate Eq. (3) where $y_2$ is forced to 0 when $y_1 = 0$ since the direction of the flow decided by splitter 2 is irrelevant when splitter 1 directs the flow towards R1-4-7 unit ($y_1 = 0$) but when $y_1 = 1$ splitter 2 can make any decision, this condition will facilitate the formulation of the subsequent constraints.

$$y_2 - y_1 \leq 0 \tag{3}$$

In this way splitters 1 and 2 also generate 3 flow paths (not 4 as without Eq. (3)) that will place some requirements on other splitters; for instance first flow path is $y_1 = y_2 = 1$, it will require that $y_9 = y_{10} = y_{11} = y_{13} = 0$; a second flow path is $y_1 = 1$ and $y_2 = 0$ which will require that $y_7 = y_9 = y_{9a} = y_{11} = y_{12} = y_{13} = 0$; and the third flow path is $y_1 = y_2 = 0$ that will require $y_9 = y_{12} = 1$ and $y_9 = y_{13} = y_{11} = 0$. These conditions will allow us to formulate Eq. (4) where only one of $y_1$ and $y_{12}$ ($y_{9a}$) variables can take the value of 1. However, in these constraints one more factor needs to be considered: if $y_{14} = 1$ the exclusive situation is necessary but when $y_{14} = 0$ there is not constraint on $y_1$, $y_{9a}$ and $y_{12}$ values (since flow has been directed to the base case configuration the values of splitters 1, 12 and 9a

are irrelevant). Eq. (5) expresses the equality among some of these variables.

$$\begin{aligned} y_1 + y_{12} + y_{14} &\le 2 \\ y_1 + y_{9a} + y_{14} &\le 2 \end{aligned} \tag{4}$$

$$y_2 = y_9 = y_{11} = y_{13} = y_7 \tag{5}$$

Relationships of splitters 1 and 2 with splitters 6 and 10 are expressed in Eq. (6).

$$\begin{aligned} y_1 - y_2 + y_6 &\le 1 \\ y_1 + y_2 - y_{10} &\le 1 \end{aligned} \tag{6}$$

Similar analysis about path flow analysis on splitters 3 and 4 generate Eq. (7) and on splitter 5 generate Eq. (8)

$$\begin{aligned} y_3 + y_4 - y_6 &\le 1 \\ y_3 &= y_8 \end{aligned} \tag{7}$$

$$y_5 = y_6 \tag{8}$$

On the potential configurations involving the base case or parts of it and analyzing the flow paths through splitters 15 and 16 the set of logical constraints is expressed in Eq. (9)

$$\begin{aligned} &y_{14} = y_{17} = y_{18} = y_{19} \\ &y_{15} = y_{16} \\ &y_6 + y_{16} - y_{15} \le 1 \\ &y_3 + y_4 + y_{15} - y_{16} \le 2 \\ &y_{16} - y_{15} - y_7 \le 0 \end{aligned} \tag{9}$$

### 4.2. Cost modeling

The objective function for the optimization is a partial cost of energy (cost per kWh). This estimation is based on the capital costs associated to some of the parts of the process, namely the gasification unit, the combined cycle power plant, and the WGS heat exchange process. To estimate this value, capital costs for the coal gasifier (including pulverization costs and air distillation unit costs), gas cleaning unit (involving ammonia and sulfur removal), pressure swing adsorber (including initial costs of the adsorption agent) were calculated using Eq. (10), where *CE* is the chemical engineering cost index (2003 value for this particular example); *A*, *B* and *C* are parameters associated to the type of equipment and *P* is a parameter related to the size of the equipment. This capital cost analysis was performed based on the cost estimation reported by the literature (Hoffman, 2005).

$$\text{Cost} = \left(\frac{CE}{A}\right) * B * \left(\frac{P}{C}\right)^{0.6} \tag{10}$$

For the WGS reactors train, the estimation of the heat exchanger capital costs was performed based on the areas of the 4-way heat exchangers and coolers and the heat duty of the heaters.

The area of the 4-way exchanger was calculated based on the constant global heat exchange coefficient provided by AEA (which extracted the individual film coefficients from the simulation) and the temperatures calculated by the Aspen Plus simulator.

The area of the coolers was calculated based on the hot fluid temperature change, the heat duty and the global heat transfer coefficients. This global heat transfer coefficient was calculated based on the individual film coefficient of the hot fluid extracted from Aspen Plus by AEA and the standard film coefficients and temperatures for the cold side (utility) employed by AEA on its economic analysis (specific for low pressure and intermediate pressure steam or for cooling tower water). The costs were calculated with Eq. (10) where *P* is the heat transfer area. It was considered that a maximum of 5000 $ft^2$ (465 $m^2$) per shell is allowed.

The costs of the heaters was estimated based on the heat load and according to the equation employed by AEA for the economics analysis (Eq. (11)) where coefficient 149.4 is employed when the heat load value is in BTU/h (155.9 when in kJ/h).

$$\text{Cost} = 100{,}000 + 149.4\left(\frac{\text{heat load}}{3600}\right)^{0.8} \tag{11}$$

In the operational costs, the utilities and the sorbent for the pressure swing absorber were included. The calculation of the cold and hot utilities was performed within the simulation.

The partial cost of energy was calculated by adding up all the capital costs and annualizing this value. The operational costs were added to the annualized capital costs and this grand total of operational costs was divided by the net generation of the plant to obtain a cost of energy in $ per KWh. This partial cost of energy can vary with the different designs formulated by AEA and with those generated by the different combinations of the 14 splitters.

## 5. Results form GBD/OA/ER/AP algorithm

### 5.1. Decomposition strategy and implicit constraints

In an equation-oriented environment, all the nonlinear equality constraints are specified explicitly. While, for a sequential modular simulator (SMS) like ASPEN, most of the constraints are implicit. This includes the black box relation between the output variables (which are part of the objective function or constraints in the master problem) and the input decision variables *x*. During the solution cycle, these implicit relations are not transferred to the master problem, resulting in a suboptimal solution. The implicit constraints can be made explicit by using additional state variables and constraints at the NLP level. This involves equating the vector of pseudovariables to the vector of output variables obtained from the flowsheet to make the black box relations transparent (Diwekar, Frey, et al., 1992; Diwekar, Grossmann, et al., 1992).

Among all the implicit variables in this superstructure (variables associated to the black-box constraints formulated by the sequential simulator), 12 cost variables were recognized as gathering information about all the other units. They were included in the MINLP problem as additional constraints shown in Eq. (12), where $O_i$ ($i = 1, \ldots, 16$) are the additional decision variables and $C_j$ ($j$ is the name of each unit) are the costs of the corresponding units which are part of the objective function. Additionally, 4 variables for splitter 14 are also included with the corresponding 4 constraints shown in Eq. (13). In these constraints $F_{14}$ is the flow at the splitter 14.

$$\begin{aligned} &O_1 - C_{\text{R1-4(1-3)}} = 0 \\ &O_2 - C_{\text{R1-4(4-6)}} = 0 \\ &O_3 - C_{\text{R1-4(7-9)}} = 0 \\ &O_4 - C_{\text{R4-10}} = 0 \\ &O_5 - C_{\text{R4-11}} = 0 \\ &O_6 - C_{\text{R4-12}} = 0 \\ &O_7 - C_{\text{R1D-4-1}} = 0 \\ &O_8 - C_{\text{STE4-1}} = 0 \\ &O_9 - C_{\text{STE4-2}} = 0 \\ &O_{10} - C_{\text{XEC1}} - C_{\text{XEC2A}} - C_{\text{XEC2B}} - C_{\text{XEC3A}} - C_{\text{XEC3B}} = 0 \\ &O_{11} - C_{\text{HE2}} = 0 \\ &O_{12} - C_{\text{HE3}} = 0 \end{aligned} \tag{12}$$

$$\begin{aligned} &O_{13} - F_{14} * y_2 = 0 \\ &O_{14} - F_{14} * (1 - y_2) = 0 \\ &O_{15} - F_{14} * (1 - y_1) = 0 \\ &O_{16} - F_{14} * (1 - y_4) = 0 \\ &O_{13} + O_{14} + O_{15} + O_{16} - F_{14} = 0 \end{aligned} \tag{13}$$

Corresponding to implicit variables, dummy constraints presented in Eq. (14) (which will be internally replaced at each iteration according to the algorithm) are included in the master

**Table 3**
Continuous decision variables information.

| Variable | Initial value | Lower bound | Upper bound |
|---|---|---|---|
| 1 (cost of unit R1-4(1–3)) | 4.7E5 | 0 | 1E10 |
| 2 (cost of unit R1-4(4–6)) | 0 | 0 | 1E10 |
| 3 (cost of unit R1-4(7-9)) | 0 | 0 | 1E10 |
| 4 (cost of unit R4-10) | 0 | 0 | 1E10 |
| 5 (cost of unit R4-11) | 55,100 | 0 | 1E10 |
| 6 (cost of unit R4-12) | 0 | 0 | 1E10 |
| 7 (cost of unit R1D-4-1) | 4.6E5 | 0 | 1E10 |
| 8 (cost of unit STE-4-1) | 2.2E6 | 0 | 1E10 |
| 9 (cost of unit STE-4-2) | 2500 | 0 | 1E10 |
| 10 (cost of units XEXC1, XEXC2A&B, XEXC3A&B) | 17,000 | 0 | 1E10 |
| 11 (cost of unit HE-2) | 0.75E6 | 0 | 1E10 |
| 12 (cost of unit HE-3) | 2E6 | 0 | 1E10 |
| 13 (flowrate of splitter 14 lb/h) | 15,000 | 0 | 1E10 |
| 14 (flowrate of splitter 14 lb/h) | 0 | 0 | 1E10 |
| 15 (flowrate of splitter 14 lb/h) | 0 | 0 | 1E10 |
| 16 (flowrate of splitter 14 lb/h) | 0 | 0 | 1E10 |
| 17 (flowrate of water to the gasifier lb mol/h) | 2800 | 0 | 4100 |
| 18 (pressure of the gasifier, psia) | 450 | 350 | 550 |
| 19 (flowrate of steam to the WGS reaction lb mol/h) | 15,000 | 0 | 1E10 |

problem. Where $X_i$ corresponds to $O_i$ for each $i$ ($i = 1, \ldots, 12$) where $U$ is a large number

$$\begin{aligned}
&X_1 - Uy_2 = 0\\
&X_2 - U(1 - y_2) = 0\\
&X_3 - U(1 - y_1) = 0\\
&X_4 - U(1 - y_3) = 0\\
&X_5 - Uy_3 = 0\\
&X_6 - Uy_4 = 0\\
&X_7 - Uy_{18} = 0\\
&X_8 - U(1 - y_5) = 0\\
&X_9 - Uy_9 = 0\\
&X_{10} - U(1 - y_{19}) = 0\\
&X_{11} - Uy_1 = 0\\
&X_{12} - U(1 - y_{14}) = 0
\end{aligned} \tag{14}$$

The initial flowsheet and three subproblems are identified from the superstructure to ensure all the units are included in the master problem. These four flowsheets are shown in Fig. 12. The binary variables corresponding to each flowsheet are given below. The constraints information that will be transferred for each subproblem is also shown below. The constraint that should link the initial flowsheet to subproblems is constraint number 17. The initial flowsheet and subproblem binary variables are given below, each of the values correspond to one of the $y_i$ ($i = 1, \ldots, 20$) splitters in Fig. 11. Also listed are the constraints affected by each subproblem.

Initial flowsheet:
$Y = (1, 1, 1, 1, 1, 1, 1, 1, 1, 0, 1, 1, 0, 1, 1, 1, 1, 1, 1, 1)$
Subproblem 1:
$Y = (1, 0, 0, 0, 0, 0, 0, 0, 0, 0, 0, 0, 0, 0, 1, 0, 0, 0, 0, 1)$
Constraints: 2, 4
Subproblem 2:
$Y = (0, 0, 0, 0, 0, 0, 0, 0, 0, 1, 0, 0, 1, 0, 1, 0, 0, 0, 0, 1)$
Constraints: 6
Subproblem 3:
$Y = (0, 0, 0, 0, 0, 0, 0, 0, 0, 0, 0, 0, 0, 0, 0, 0, 0, 0, 0, 0)$
Constraints: 10

There are three continuous decision variables (other than the 16 variables created to handle the implicit constraint situation) that are selected to obtain an optimal design. These variables are: mole flow water that is fed to the gasifier which is linked to its temperature, the mole flow of steam that is mixed with the flue gases prior the WGS reactor and determines the steam to CO ratio, and the gasifier pressure. These variables were evaluated and analyzed with respect to energy costs (Hoffman, 2005); however, in that work each variable was analyzed separately. The conclusions of the study resulted in the suggestion that decreasing water intake, keeping the base case pressure and decreasing steam flowrate for the WGS would reduce the energy costs. For this reason, the lowest possible water intake for the gasifier, the base case pressure and a slightly smaller steam flowrate were chosen as base case in the present study. The bounds and initial values of all the continuous variables are shown in Table 3.

### 5.2. Optimization results

After all MILP and NLP iterations of the GBD/OA/ER/AP algorithm the results of this exercise are shown in Table 4. It should be noted that only the three real decision variables (variables 17, 18, and 19) are reported here as the first 16 variables correspond to implicit constraint variables.

As noted the base case cost was 7.98E−02. This exercise obtained a solution which is 26% less expensive than the base case. Further, there is a large number of combinations that are possible with this superstructure, but to find the optimal solution (second row of Table 4) the GBD/OA/ER/AP algorithm only took 2 MINLP iterations (28 NLP iterations, 112 model runs in total) to find the solution.

## 6. Results from simulated annealing algorithm

### 6.1. Optimization results

The optimal binary variables obtained by SA the same base configuration (all values of y values were equal to zero), and the objective function is found to be 5.77E−2 which is less than the MINLP solution. The optimal values of the three decision variables are found to be 3225 lb mol/h (1462 kmol/h), 362.5 psia (25 bar), and 33,333 lb mol/h (15,120 kmol/h) for the gasifier water inlet, gasifier pressure, and WGS reaction water inlet, respectively.

## 7. Discussion

The two solutions are summarized in Fig. 13. It is noted that both solutions found the same configuration. However, the continuous variables are different for the two solutions. This can be attributed to the fact that the solution space is non-convex. Therefore, SA could find better solution than the GBD/OA/ER/AP algorithm.

Solution obtained with SA algorithm is counterintuitive. Water flow rate fed to the gasifier is increased which implies decreasing

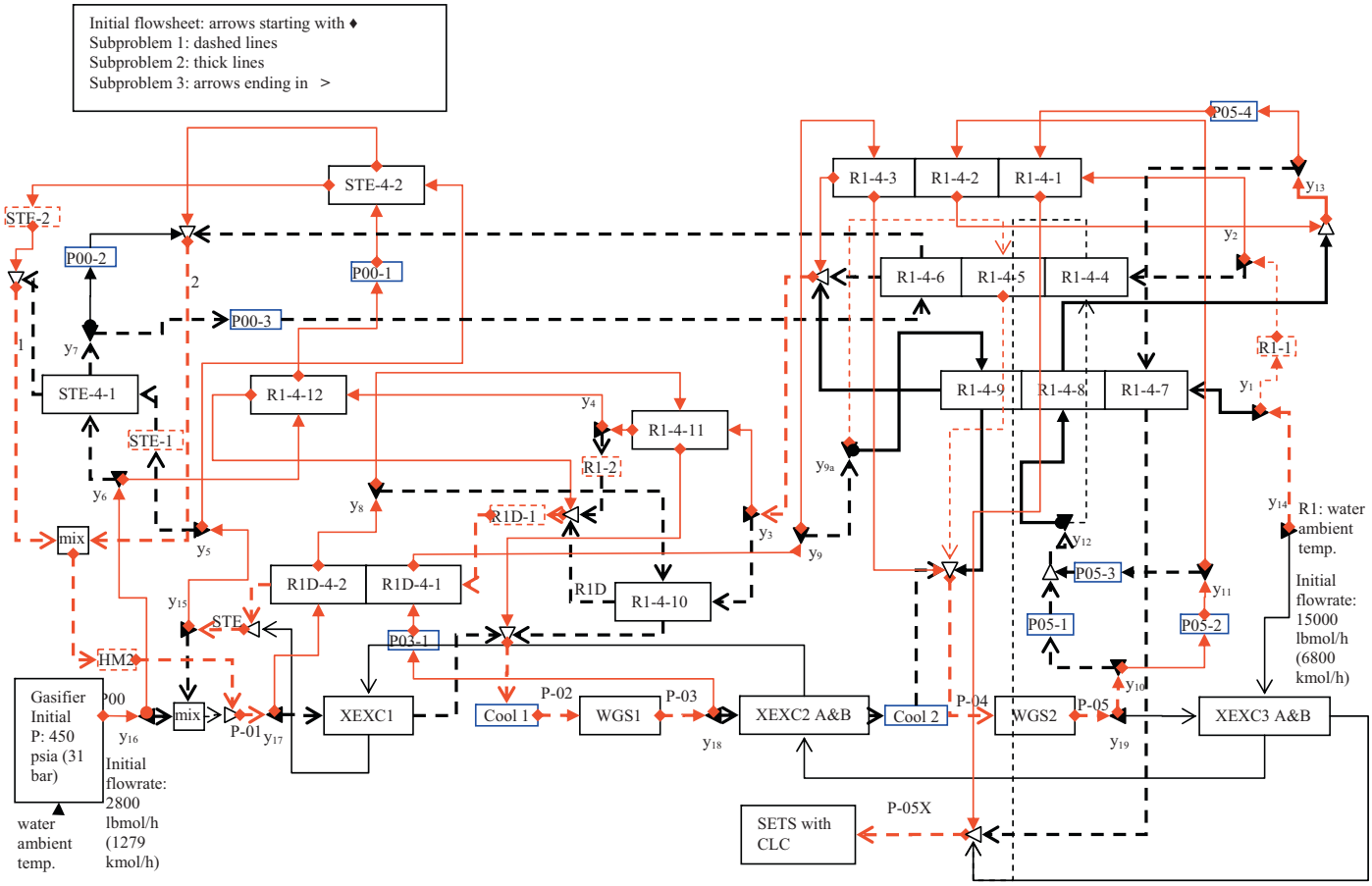


**Fig. 12.** Initial flowsheet and subproblems for the GBD/OA/ER/AP algorithm. Use the same kew as in Fig. 11 for unit operations and splitters.

**Table 4**
Results of the solution for the MINLP problem.

| Iteration of MILP (master problem) | Solution of MILP (master problem) | Solution of NLP (secondary problems) |
|---|---|---|
| 1 | $y = (1, 1, 1, 1, 1, 1, 1, 1, 1, 0, 1, 1, 0, 1, 1, 1, 1, 1, 1, 1)$ | OPTVAR(17–19) = (2784.6, 449.59, 39832) Obj. Function = 6.70E−02 |
| 2 | $y = (0, 0, 0, 0, 0, 0, 0, 0, 0, 0, 0, 0, 0, 0, 0, 0, 0, 0, 0, 0)$ | OPTVAR(17–19) = (2800.0, 450.00, 15000) Obj. Function = 5.94E−02 |
| 3 | INFEASIBLE: solution reached | |

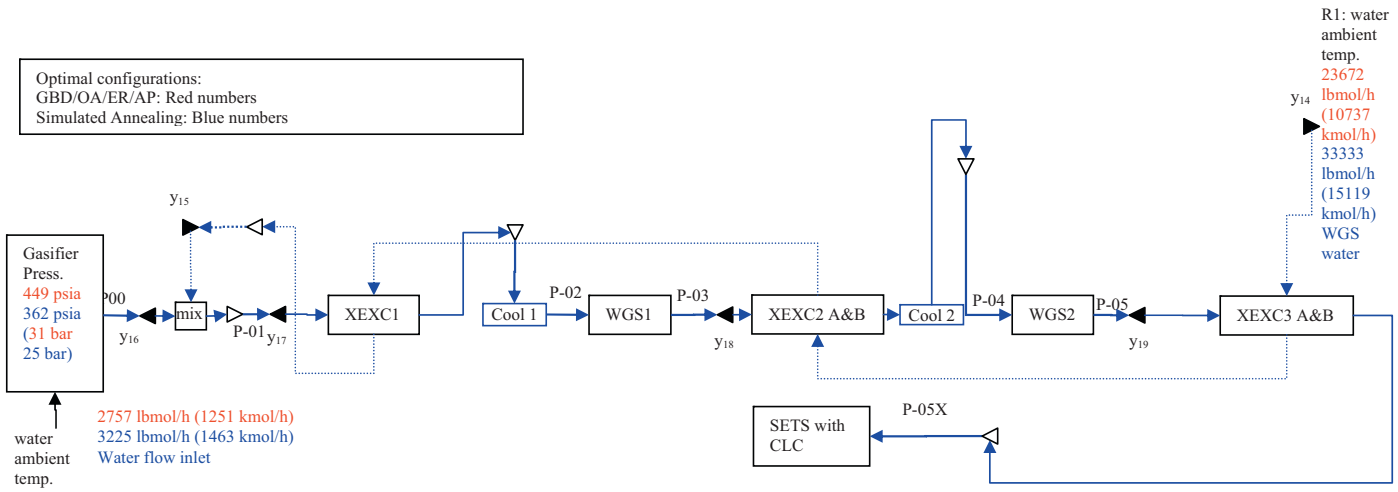


**Fig. 13.** Optimal solutions obtained with two MINLP algorithms.

gasifier temperature and reduction of the cooling requirements, this action reduces the heat exchange area and utility consumption and it is complemented with an increase in water flow rate for the WGS drastically reducing the costs since the heat exchange area is reduced. However, the payoff of this low costs is that the steam mixed with the gas stream is not saturated, it still contains some liquid, and this may imply operational difficulties.

## 8. Conclusion

Process synthesis is necessary when new technologies are invented to satisfy energy generation needs. One of these needs is carbon capture which can be favored by employing efficient post-gasification techniques such as water–gas shift (WGS) reaction and sorbent energy transfer system (SETS) based on chemical looping combustion. Heat integration is an important part of process synthesis and Aspen Energy Analyzer (AEA) can provide alternative designs. However, these designs are based on linear models that need to be validated by Aspen Plus simulations. A considerable difference between the AEA prediction and those results from Aspen Plus simulations was observed. Employment of the Aspen Plus simulation guarantees that the downstream conditions are kept under the process requirements and heat exchangers are evaluated with reliable models in order to evaluate possible configurations generated by AEA. An MINLP problem can be formulated by creating and simulating a superstructure with those alternative designs. An optimal design was found employing two different algorithms for an IGCC system with new technologies for carbon capture. These two algorithms provided two different solutions but same configuration. Simulated annealing algorithm provided a solution which is slightly better than GBD/OA/ER/AP. However, this solution may pose a practical problem. The approach presented here can be used for any real world process synthesis problem.

## References


Diwekar, U. (2010a). *User manual for CAPE-OPEN Mixed Integer Non-linear Programming (MINLP) capability. This manual can be obtained by writing to the author.*

Diwekar, U. (2010b). *User manual for CAPE-OPEN simulated annealing capability. Manual can be obtained by writing to the author.*

Diwekar, U. M. (2008). *Introduction to applied optimization* (2nd ed.). New York: SpringerLink.

Diwekar, U. M., Frey, H. C., & Rubin, E. S. (1992). Synthesizing optimal flowsheets: Applications to IGCC system environmental control. *Industrial and Engineering Chemistry Research*, *31*, 1927–1936.

Diwekar, U. M., Grossmann, I. E., & Rubin, E. S. (1992). An MINLP process synthesizer for a sequential modular simulator. *Industrial and Engineering Chemistry Research*, *31*, 313–322.

Diwekar, U. M., & Rubin, E. S. (1993). Efficient handling of the implicit constraints problem for the ASPEN MINLP synthesizer. *Industrial and Engineering Chemistry Research*, *32*, 2006–2011.

Doctor, R. D., Molburg, J. C., & Thimmapuram, P. R. (1996). KRW oxygen-blown gasification combined cycle: Carbon dioxide recovery. *Transport and Disposal*, *ANL/ESD-34*, 177.

Domenichini, R., Gallio, M., & Lazzaretto, A. (2010). Combined production of hydrogen and power from heavy oil gasification: Pinch analysis, thermodynamic and economic evaluations. *Energy*, *35*, 2184–2193.

El-Sayed, Y. M. (1999). Revealing the cost-efficiency trends of the design concepts of energy-intensive systems. *Energy Conversion and Management*, *40*, 1599.

Emun, F., Gadalla, M., Majozi, T., & Boer, D. (2010). Integrated gasification combined cycle (IGCC) process simulation and optimization. *Computers and Chemical Engineering*, *34*, 331–338.

Farhad, S., Saffar-Avval, M., & Younessi-Sinaki, M. (2008). Efficient design of feedwater heaters network in steam power plants using pinch technology and exergy analysis. *International Journal of Energy Research*, *32*, 1–11.

Gadalla, M., Emun, F., Majozi, T., & Jiménez, L. (2009). Environmental design of IGCC through pinch analysis, process integration and parameters analysis. In Jacek Jeżowski, & Jan Thullie (Eds.), *Computer aided chemical engineering* (pp. 561–566). Elsevier.

Harkin, T., Hoadley, A., & Hooper, B. (2009). Process integration analysis of a brown coal-fired power station with $CO_2$ capture and storage and lignite drying. *Energy Procedia*, *1*, 3817–3825.

Hoffman, Z. (2005). *Simulation and economic evaluation of coal gasification with SETS reforming process for power production*.

Kalagnanam, J. R., & Diwekar, U. M. (1997). An efficient sampling technique for off-line quality control. *Technometrics*, *39*, 308–320.

Linhoff, B., & Alanis, F. J. (1989). A systems approach based on pinch technology to commercial power station design. *ASME Advanced Energy Systems*, *85*, 10–15.

Linhoff, B., Townsend, D. W., Boland, D., Hewitt, G. F., Thomas, B. E. A., Guy, A. R., et al. (1982). *A user guide on process integration for efficient use of energy*. Rugby, Warks, England: The Institution of Chemical Engineers.

Madzivhandila, V., Majozi, T., & Zhelev, T. (2009). Process integration as an optimization tool in clean coal technology: A focus on IGCC. *Chemical Engineering Transactions*, *18*, 941–946.

Vlaswinkel, E. E. (1992). Energetic analysis and optimization of an integrated coal gasification-combined cycle power plant. *Fuel Processing Technology*, *32*, 47–67.

Wang, Y., Qiu, P., Wu, S., & Li, Z. (2010). Performance of an integrated gasification combined cycle system with different system integration options. *Energy Fuels*, *24*, 1925–1930.

Yu, J., Corripio, A. B., Harrison, D. P., & Copeland, R. J. (2003). Analysis of the sorbent energy transfer system (SETS) for power generation and $CO_2$ capture. *Advances in Environmental Research*, *7*, 335–345.